

GEO and LEO: The Final Frontier for Plutonic FFP Parallax

ANDREW GOULD^{1,2}

¹*Department of Astronomy, Ohio State University, 140 W. 18th Ave., Columbus, OH 43210, USA*

²*Max-Planck-Institute for Astronomy, Königstuhl 17, 69117 Heidelberg, Germany*

ABSTRACT

I show that microlens parallaxes, π_E , can be derived for free-floating planets (FFPs) with masses down to that of Pluto, by combining observations from a satellite in geosynchronous (GEO) orbit with another observatory that is on or near Earth’s surface, i.e., either ground-based or in low Earth orbit (LEO). Because these low-mass FFPs typically have measurements of the angular Einstein radius, θ_E , from finite-source effects, such π_E measurements directly yield the FFP mass $M = \theta_E/\kappa\pi_E$ where κ is a physical constant. Such Earth-GEO measurements almost perfectly complement Earth-L2 measurements, which extend to higher FFP mass and greater FFP distance. LEO-only observations can yield mass measurement at even smaller FFP mass and nearer FFP distances. I discuss methods for breaking the Refsdal (1966) two-fold degeneracy in $\pi_{E,\pm}$.

Subject headings: gravitational lensing; micro

1. Introduction

It is at least plausible that there is a vast population of sub-planetary objects that can generate free-floating planet (FFP) type signals, i.e., brief, single-lens single-source (1L1S) microlensing events that show no trace of a host. Both Gould et al. (2022) and Sumi et al. (2023) derived FFP mass functions that were consistent with $dN/d\log M \propto M^{-1}$, i.e., equal mass of planetary material per logarithmic bin, albeit with large statistical uncertainties. In particular, Gould et al. (2022) noted that if this power law were extended by 18 orders of magnitude, it would also be consistent with observations of interstellar asteroids and comets.

While FFPs may be truly “free” (i.e., not bound to any star), they may also simply be so far from their hosts that these hosts do not leave any trace on the event. Gould (2016) discussed how to distinguish these two classes, and indeed how to further divide the bound

FFPs into various subclasses, and Gould et al. (2024) examined this issue in greater detail. In particular, Gould et al. (2024) pointed out that if the host can be identified, then the FFP mass can be measured using a slight variant of the method originally proposed by Refsdal (1964):

$$M = \frac{\theta_E^2}{\kappa\pi_{\text{rel}}} = \frac{(\mu_{\text{rel}}t_E)^2}{\kappa\pi_{\text{rel}}}; \quad \kappa \equiv \frac{4G}{c^2\text{au}} = 8144 \frac{\mu\text{as}}{M_\odot}, \quad (1)$$

where $(\pi_{\text{rel}}, \mu_{\text{rel}})$ are the lens-source relative (parallax, proper motion) and (θ_E, t_E) are the Einstein (angular radius, timescale),

$$\theta_E \equiv \sqrt{\kappa M \pi_{\text{rel}}}; \quad t_E \equiv \frac{\theta_E}{\mu_{\text{rel}}}. \quad (2)$$

That is, once the host is identified, the host-source relative parallax can be measured, and this is the same as the lens-source relative parallax, π_{rel} . Moreover, even if θ_E is not measured from the event, it can be determined from two epochs of host-source astrometry, which yield the host-source relative proper motion, which is essentially the same as lens-source relative proper motion, μ_{rel} . Because t_E is measured during the event, this immediately yields $\theta_E = \mu_{\text{rel}}t_E$.

On the other hand if the FFP is unbound (or if the host cannot be identified), then the only way to determine the mass is to measure the microlens parallax,

$$\boldsymbol{\pi}_E \equiv \pi_E \frac{\boldsymbol{\mu}_{\text{rel}}}{\mu_{\text{rel}}}; \quad \pi_E \equiv \frac{\pi_{\text{rel}}}{\theta_E} = \sqrt{\frac{\pi_{\text{rel}}}{\kappa M}}. \quad (3)$$

Then,

$$M = \frac{\theta_E}{\kappa\pi_E}. \quad (4)$$

Moreover, if the FFP is in the bulge, then (even if it is bound to an identified host) the Refsdal (1964) method of Equation (1) will likely lead to a very uncertain mass estimate because $\pi_{\text{rel}} = \pi_l - \pi_s$ is the difference of two very similar quantities.

Thus, obtaining microlens parallax measurements for FFPs is crucial for understanding this population.

The main focus for FFP microlens parallax measurements has been on L2 parallaxes, whereby the event is observed simultaneously from the ground and L2 (Gould et al. 2003; Zhu & Gould 2016; Gould et al. 2021; Ge et al. 2022), from two satellites in different L2 orbits (Bachelet & Penny 2019; Ban 2020; Gould et al. 2021; Bachelet 2022) or from L2 and low-Earth-orbit (LEO, Yan & Zhu 2022). There are two main reasons for this focus on L2, one theoretical and the other practical.

The theoretical reason is that to successfully employ the two-observatory method to measure parallax that was originally proposed by Refsdal (1966), the magnitude of the projected separation of the two observatories, $D_{\perp} = |\mathbf{D}_{\perp}|$, must be approximately matched to the projected Einstein radius of the target population,

$$\tilde{r}_{\text{E}} \equiv \frac{\text{au}}{\pi_{\text{E}}} = \text{au} \sqrt{\frac{\kappa M}{\pi_{\text{rel}}}} = 0.02 \text{ au} \left(\frac{M}{M_{\oplus}} \right)^{1/2} \left(\frac{\pi_{\text{rel}}}{60 \mu\text{as}} \right)^{-1/2}, \quad (5)$$

In the Refsdal (1966) method, the Paczyński (1986) parameters (t_0, u_0, t_{E}) of the event from each of the two observatories are measured, and $\boldsymbol{\pi}_{\text{E}}$ is inferred by

$$\boldsymbol{\pi}_{\text{E}} = (\pi_{\text{E},\parallel}, \pi_{\text{E},\perp}) = \frac{\text{au}}{D_{\perp}} (\Delta\tau, \Delta\beta); \quad \Delta\tau \equiv \frac{t_{0,1} - t_{0,2}}{t_{\text{E}}}; \quad \Delta\beta \equiv u_{0,1} - u_{0,2}. \quad (6)$$

Thus, if $D_{\perp} \ll \tilde{r}_{\text{E}}$, then the two observatories will see essentially the same event, while if $D_{\perp} \gg \tilde{r}_{\text{E}}$, then one of the two observatories will not see the event at all. Gould et al. (2024) argued that at a given D_{\perp} , one could approximately probe the range of \tilde{r}_{E} satisfying

$$0.05 \lesssim \frac{D_{\perp}}{\tilde{r}_{\text{E}}} \lesssim 2. \quad (7)$$

In their Figure 4, they showed that this factor ~ 40 range in \tilde{r}_{E} (factor $40^2 = 1600$ in mass) is approximately centered on M_{\oplus} for L2 (i.e., $D_{\perp} \simeq 0.01 \text{ au}$) separations and for the typical range of π_{rel} that characterizes microlensing events seen toward the Galactic bulge. See also Figure 1, below. As M_{\oplus} FFPs have been the first focus of interest for next-generation microlensing experiments, L2 separations appear to be ideal.

The practical reason is that the *Roman* and *Euclid* survey telescopes will operate (or already are operating) in L2 orbits. *Roman* will have a very large microlensing component, while *Euclid* may adopt one later in its mission. In addition, the *Earth 2.0 (ET)* mission is specifically designed to acquire Earth-L2 parallax measurements.

The main point of Gould et al. (2024) was that by adjusting its observation schedule, *Roman* could be made much more sensitive to Pluto-mass FFPs, i.e., $M \sim 0.002 M_{\oplus}$. Although these are individually more difficult to detect than Earth-mass FFPs, they could plausibly be ~ 500 times more numerous, and hence a radically different FFP population could be effectively probed. However, their same Figure 4, which showed that L2 separations are extremely well-matched to Earth-mass FFP parallaxes, also shows (unsurprisingly) that they are poorly matched to Pluto-mass FFP parallaxes. In particular, for Plutos with sufficiently large $\pi_{\text{rel}} \gtrsim 60 \mu\text{as}$ to be detected at all, the observatories are too far apart to both observe the same FFP event. While it would still be of great interest just to detect these Plutos, this mismatch raises the question of whether it is possible to measure the $\boldsymbol{\pi}_{\text{E}}$ for this potentially very numerous class of objects.

Here I discuss two approaches to tackling this challenge.

2. Two Channels of Microlens Parallax

Refsdal (1966) and Gould (1992) charted two logically distinct channels to measure π_E , i.e., simultaneous observation from two platforms, and observation from a single accelerated platform, respectively. In the original Refsdal (1966) approach, the two platforms were the Earth and a satellite in solar orbit, so a baseline $D_\perp \sim \mathcal{O}(\text{au})$. However, Holz & Wald (1996) proposed to apply the same two-observatory concept on an $\epsilon_{\text{TP}} \sim 1/23,500$ times smaller scale by placing both observatories on Earth (“terrestrial parallax”, TP), while Gould et al. (2003) proposed to apply it on an $\epsilon_{\text{L2}} \sim 1/100$ smaller scale by placing the observatories on Earth and at L2, as described in Section 1. Given the $\tilde{r}_E \propto M^{1/2}$ scaling of Equation (5), one might expect these to have peak sensitivities that are smaller than the original Refsdal (1966) proposal by factors of $\epsilon_{\text{TP}}^2 = 2 \times 10^{-9}$ and $\epsilon_{\text{L2}}^2 = 10^{-4}$, respectively. Because the peak sensitivity¹ for a satellite at 1 au is actually $M_{\text{peak,au}} \sim 0.04 M_\odot$, these scaling relations predict $M_{\text{peak,TP}} = \epsilon_{\text{TP}}^2 M_{\text{peak,au}} \sim 3 \times 10^{-5} M_\oplus$ and $M_{\text{peak,L2}} = \epsilon_{\text{L2}}^2 M_{\text{peak,au}} \sim 1.3 M_\oplus$, respectively. Comparing to the discussion in Section 1, we see that this naive reasoning accurately predicts the application that has been envisaged for L2. However, it seems to predict that the utility of TP will be centered on unobservably small objects. In fact, the two TP events observed to date (Gould et al. 2009; Yee et al. 2009) have been much more massive, but this is because they were extreme magnification events, as predicted by Gould (1997).

The second channel is to observe the event from a single observatory on an accelerated platform. The first such platform was Earth itself (Gould 1992), which yields so-called “annual parallax” (AP), but this was soon followed by “low-Earth orbit (LEO) parallax” (Honma 1999) and “geosynchronous orbit parallax” (GEO, Gould 2013a).

The spatial scale of LEO is the same as TP, i.e., R_\oplus , and thus (just as in TP) the practical application presented by Honma (1999) relied on sharply peaked magnification structures, in this case, caustics, to have a measurable effect.

The spatial scale and time scale of GEO are $a_{\text{GEO}} \sim 6.6 R_\oplus$ and $P_{\text{GEO}} = 1 \text{ d}$, which would seem to be ill-matched to the requirements of acceleration-based parallax measurements. To illustrate their feasibility, Gould (2013a), chose an event with a typical Einstein timescale, $t_E = 20 \text{ d}$, but an effective timescale matched to the orbital period, $t_{\text{eff}} \equiv u_0 t_E = P_{\text{GEO}}$, i.e., with $u_0 = 0.05$. In this way, the parallax displacement was amplified by $A_{\text{max}} = 20$ over an orbital period, to $\delta \ln A \sim \delta u / u_0 \sim \pi_E A_{\text{max}} a_{\text{GEO}} / \text{au} = \pi_E 20 (2.8 \times 10^{-4}) \rightarrow 8 \times 10^{-4}$, where

¹For this purpose, I define the “peak” according to the geometric means of the limits of Equation (7), i.e., the point at which $\tilde{r}_E = D_\perp \sqrt{10}$, and evaluated at the mid-point of the abscissa of Figure 4 from Gould et al. (2024), i.e., $\log(\pi_{\text{rel}}/\mu\text{as}) = 1.5$, or $\pi_{\text{rel}} = 32 \mu\text{as}$. Substituting $D_\perp = 1 \text{ au}$, Equation (5) then yields $M = 0.04 M_\odot$.

$\pi_E \sim 0.14$ was the value chosen by Gould (2013a) for the illustration. Nevertheless, Gould (2013a) argued that these small oscillations could be reliably measured, in part because they repeated over several days, and in part because there would be a rigorous, and very precise, check from AP on one of the two π_E components that were derived from these oscillations. See his Figures 2 and 3.

Subsequently, Mogavero & Beaulieu (2016), showed that GEO observations were well matched to the task of measuring π_E for $t_E \sim P_{\text{GEO}} = 1$ d, i.e., Jupiter-class FFPs and very low mass brown dwarfs.

These examples illustrate that while the overall scaling relations provide a useful guide, the concrete circumstances of each application must be closely considered.

3. New Application of GEO to Dwarf-Planet Parallaxes

Pluto is 456 times less massive than Earth. Hence, the peak sensitivity for Pluto-mass objects should be achieved at projected separations, D_\perp that are $\sqrt{456} \simeq 21.4$ times smaller than for Earth-mass objects, i.e., $D_\perp = 0.01 \text{ au}/21.4 = 11.0 R_\oplus$, just 1.7 times larger than a GEO orbit. Given that the mass sensitivity spans several decades centered on this peak, this factor 1.7 is quite minor. The first incarnation of this idea, i.e., separate observatories on Earth and in GEO, is qualitatively different from the GEO approach proposed by Gould (2013a) and further explored by Mogavero & Beaulieu (2016), which made use of a single accelerated observatory at GEO and which was discussed in Section 2.

I illustrate the sensitivity of this approach in Figure 1, which is a version of Figure 4 from Gould et al. (2024) that has been extended to include GEO parallaxes in addition to L2 parallaxes. The gray lines show the parallax limits of Equation (7) as applied to GEO ($D_\perp = 6.63 R_\oplus$), just as the red lines show these limits as applied to L2 ($D_\perp = 0.01 \text{ au}$). The magenta (“Paczynski Limit”) and blue (“Detection Limit”) lines are exactly the same as in Figure 4 of Gould et al. (2024). The Paczynski Limit requires that $\rho \equiv \theta_*/\theta_E < 2$ so that the Paczynski (1986) parameters, u_0 and t_E , which are needed for Equation (6), can be measured. Johnson et al. (2022) showed that this becomes increasingly difficult for $\rho \gg 1$. In particular, the gray contours outline the region of M - π_{rel} space that is accessible to GEO parallaxes, just as the green contours outline the region of M - π_{rel} space that is accessible to L2 parallaxes. Notably, the two regions slightly overlap, so that their union covers a vast swath of this space down to the Paczynski limit. One observes that Moon-mass objects are accessible to GEO parallaxes for the “outer disk”, i.e., $D_L \lesssim 5 \text{ kpc}$, while Pluto-mass objects are accessible for the “nearby” population, $D_L \lesssim 1.3 \text{ kpc}$. By comparison, such objects are

completely inaccessible to L2 parallaxes, regardless of lens distance.

However, Figure 1 contains a hidden assumption, namely that early M-dwarf sources, with $\theta_* = 0.3 \mu\text{as}$ are observable. That is, the Paczyński limit shown in Figure 1 is based on $\theta_* = 0.3 \mu\text{as}$, as being “typical” of *Roman* sources. But for parallax to be measured, the same sources must be accessible to the other observatory. Gould et al. (2024) considered various possibilities for the second observatory, such as *Euclid* (also in L2), *CSST* in LEO, as well as observatories on Earth. Their Figure 4, showed only the most favorable case for L2 parallaxes. Regarding GEO parallaxes, perhaps such early M-dwarf sources could be reached with LSST, and so Figure 1 could be considered relevant to them. For example, the GEO satellite could be placed over the Western Pacific, so that D_\perp could be near its maximum value when the Galactic bulge is near zenith in Chile. Then, other, less powerful observatories could be placed in Africa, which would take advantage of complementary diurnal time periods. Note that because the bulge fields have Declination, $\delta \sim -29^\circ$, while GEO orbits are on the equator, the minimum value of D_\perp during the daily GEO cycle is approximately $D_{\perp,\text{min}} \sim a_{\text{GEO}} \sin |\delta| \sim a_{\text{GEO}}/2$, depending on the precise position of the observatory on Earth.

Whether or not LSST could be convinced to undertake such dedicated observations (see Gould 2013b), one therefore should also consider less capable observatories, i.e., either working to complement LSST (as above) or instead of it. To this end, I show in Figure 2, a second view of the same parameter space, but adopting $\theta_* = 0.48 \mu\text{as}$, which would be more accessible from typical ground-based surveys. One sees that regions of the Galaxy in which Moon-mass and Pluto-mass objects are detectable contracts significantly, although both are still detectable at some lens distances. Mathematically, the lower limit on π_{rel} (at fixed M) increases by a factor $(0.48/0.30)^2 = 2.56$ between the two diagrams, which is ~ 0.4 dex, i.e., 2 tic marks on the abscissa.

Another possibility for the second observatory would be a satellite in LEO. This would have the advantage of space quality photometry and would yield essentially the same D_\perp as the ground-based observatories discussed above. Such a LEO survey telescope, namely the *Chinese Space Station Telescope (CSST)* is already being planned by the National Astronomical Observatories of China. Compared to Earth-bound telescopes, a LEO observatory has the important advantage of permanent good weather. It can also observe the bulge for a greater fraction of the 8760 hours of the year, being only restricted by the horizon and the time that Sun is not in/near the bulge², rather than scattered sunlight in Earth’s atmosphere.

²Depending on the phase of the 19-year Metonic cycle and the baffling of the telescope, the Moon may interfere with observations as well. This will also be more severe for ground-based than LEO observatories.

A more ambitious option would be to place two telescopes in GEO, for example, separated in phase by 180° . In this case D_\perp would oscillate between $2 a_{\text{GEO}}$ and $2 \sin |\delta| a_{\text{GEO}} = 0.97 a_{\text{GEO}}$ over every 12 hours. Observations could be continuous except when the Sun was in or near the Galactic bulge. That is, even when Earth and the bulge were most closely aligned, the line of sight toward the bulge would pass $(\sin \delta) a_{\text{GEO}} - R_\oplus \simeq 2.21 R_\oplus$ from Earth’s surface. Or, expressed in terms of angle, $\psi = |\delta| - \sin^{-1}(R_\oplus/a_{\text{GEO}}) \simeq 20.3^\circ$.

We can use Figure 1 to gauge the sensitivity to low-mass planets and dwarf planets. At minimum separation, $D_\perp \simeq a_{\text{GEO}}$, which is almost exactly what is represented in Figure 1. At maximum separation, $D_\perp = 2 a_{\text{GEO}}$, so that the cyan lines would be moved upward by a factor 4 (i.e., 0.6 dex, slightly more than 1 tic mark) relative to Figure 1. Hence, considering all phases of the orbit, there would be a broad range of sensitivity to planets from Earth-mass to Pluto-mass.

4. How to Break the Refsdal Parallax Degeneracy

As already pointed out by Refsdal (1966) (see also Figure 1 of Gould 1994), Equation (6) does not lead to a unique solution because u_0 is a signed quantity, but generally only its amplitude can be derived from a microlensing light curve. And this is particularly the case for very short events, which are the sole object of interest in the present context.

This issue is of exceptional importance for low-mass FFPs because the main statistical argument, the so-called “Rich argument” for breaking this degeneracy may not apply to them. I explain both the argument and its potential problems via a concrete example.

Suppose that $D_\perp = 6 R_\oplus$, $\theta_* = 0.3 \mu\text{as}$, $\rho = 1$, $u_{0,1} = 0.35$, $u_{0,2} = 0.4$, $t_E = 0.66 \text{ hr}$, $\Delta\tau = 0.05$. I first note that, independent of any issue related to parallax, $\theta_E = \theta_*/\rho = 0.3 \mu\text{as}$, and $\mu_{\text{rel}} = \theta_E/t_E = 4.0 \text{ mas yr}^{-1}$. Now, according to Equation (6), there are four possible values of $\Delta\beta$, i.e., $\pm(0.4 - 0.35) = \pm 0.05$ and $\pm(0.4 + 0.35) = \pm 0.75$. Therefore, there are two possible values of $\sqrt{(\Delta\tau)^2 + (\Delta\beta)^2}$, namely $\sqrt{0.05^2 + 0.05^2} \simeq 0.071$ and $\sqrt{0.05^2 + 0.75^2} \simeq 0.75$, and therefore two values of the parallax, $\pi_{E,-} = 279$ and $\pi_{E,+} = 2950$. These then lead to two pairs of values for (M, π_{rel}) , namely $(M/M_\oplus, \pi_{\text{rel}}/\mu\text{as})_- = (0.044, 84)$ and $(M/M_\oplus, \pi_{\text{rel}}/\mu\text{as})_+ = (0.0042, 885)$. These correspond to a Mercury-mass object at $D_L \sim 5 \text{ kpc}$ and a 2-Pluto-mass object at $D_L \sim 1 \text{ kpc}$. According to the formal statement of the Rich argument (Gould 2020), the first solution is strongly favored by several factors, including that there is 125 times more volume at 5 times the distance, as well some Jacobian factors. Therefore, in typical circumstances, one would just “choose” the $\pi_{E,-}$ solution as being overwhelmingly probable. Of course, this would lead to occasional mistakes, but these

would not affect any overall statistical conclusions.

However, in the present case, it could be that Pluto-class objects are 10 or even 100 times more common than Mercury-class objects. If the relative frequency were known to be very high, then this procedure might lead to an ambivalent conclusion about this particular object, despite the strong support for the Mercury-mass conclusion from the geometric components of the Rich argument. However, the real issue is that we do not know this relative frequency a priori, and we have no means to determine it except from this, and similar, experiments. Therefore it is important to try to resolve the Refsdal (1966) degeneracy using data and not simply statistical arguments.

Two of the methods described in Section 3 provide paths toward such resolution.

If the second observatory is in LEO, then there will be a very strong signal for the 2-Pluto-mass solution because $\tilde{r}_{E,+} = au/\pi_{E,+} = 8 R_{\oplus}$, i.e., just 8 times larger than the orbit. On the other hand, for the Mercury-mass solution, $\tilde{r}_{E,-} = 85 R_{\oplus}$, so the parallax signal would be unmeasurably small. Note that in the example given, u remains $u < 1.5$ for an interval $\delta t = 2.89 t_E = 1.9$ hr, (substantially more than the 90 min orbital period), during which time the magnification, A , remains $A(u) = (u^2 + 2)/u\sqrt{u^2 + 4} > 17/15$. Therefore, the parallax signal is clearly detectable despite the roughly 50 min gap in the data due to Earth occultation. The signal becomes more difficult to recover for cases that the magnification does not remain significant on both sides of an Earth occultation.

If the second observatory is also in GEO, then this opens the possibility of the “3-observatory” method of resolving the Refsdal (1966) two-fold degeneracy, $\pi_{E,\pm}$. This has actually been done for three cases, OGLE-2007-BLG-224 (Gould et al. 2009), OGLE-2008-BLG-279 (Yee et al. 2009), and MOA-2016-BLG-290 (Zhu et al. 2017). The first two were TP measurements, with all three observatories being on Earth. The last was simultaneously observed from Earth and by the *Spitzer* and *Kepler* satellites. A crucial fact about this method is that the third-observatory measurement can be of much lower quality than the other two because it does not need to independently determine the parameters of the event, but only break the degeneracy between the implications from the two other measurements. For example, in the case of OGLE-2007-BLG-224, the degeneracy-breaking measurements from the Liverpool Telescope (Canaries) contained only points $\gtrsim 2$ mag below the peak. Nevertheless, when combined with knowledge of t_E from other observatories, these determined $t_{0,\text{Canaries}}$ to a precision of < 3 s, even though these data, by themselves, contained essentially no information about $u_{0,\text{Canaries}}$.

Taking note of this fact, one could augment the system of two GEO observatories (with 180° relative phase) by a much less capable observatory (or set of observatories with

near-continuous capability) on Earth. For simplicity, consider the idealized situation that the Earth observations take place from Earth’s center. Then, if we label the projected positions of the three observatories \mathbf{A}_\perp , \mathbf{B}_\perp , and \mathbf{C}_\perp (with Earth being the last), we obtain $\mathbf{C}_\perp = (\mathbf{A}_\perp + \mathbf{B}_\perp)/2$. And therefore $t_{0,\mathbf{C}} = (t_{0,\mathbf{A}} + t_{0,\mathbf{B}})/2$ and $u_{0,\mathbf{C}} = (u_{0,\mathbf{A}} + u_{0,\mathbf{B}})/2$. The two degenerate solutions yield the same values of t_0 , so the first of these two equations is not useful. However, the second can make very different predictions for u_0 . In the present case $|u_{0,-,\mathbf{C}}| = 0.025$, while $|u_{0,+,\mathbf{C}}| = 0.375$. Note that allowing the Earth observatory to operate from its surface (rather than its center) changes the mathematical details of this example, but not the basic principle.

5. LEO-only Observatory

The manner in which the LEO observatory can break the degeneracy between the two ($\pi_{\mathbf{E},\pm}$) solutions derived from Earth+GEO observations (Section 4), raises the possibility that LEO-only observations could measure $\pi_{\mathbf{E}}$ by itself, i.e., with no help from a second observatory (Mogavero & Beaulieu 2016). Clearly, the domain of such measurements would be much more restricted than the GEO option that is illustrated in Figure 1. For example, as just recounted in Section 4, the Mercury-mass FFP at $D_L \sim 5$ kpc. would have an unmeasurably small parallax signal from LEO, whereas it would be easily detectable using Earth+GEO. On the other hand, the 2-Pluto-mass FFP at $D_L \sim 1$ kpc could be characterized from LEO alone.

However, the overall prospects for such a LEO observatory cannot be properly evaluated using the analytic techniques of the present work: there are several interrelated issues that can only be addressed using simulations. One such issue has already been described, namely the effect of the windowing of the observations by Earth occultations. To help understand the other issues, I present in Figure 3, a LEO-style version of Figure 1, which is calculated by replacing $D_\perp = a_{\text{GEO}}$ with $D_\perp = a_{\text{LEO}} \rightarrow R_\oplus$. This substitution is not strictly kosher, exactly because the resolution of the issues raised in this section could alter some features of this diagram and/or the interpretation of these features. Nevertheless, the Figure is useful because it permits us to frame the discussion of these issues.

The second issue is the rapidly changing μ_{rel} distribution for lens distances $D_L \lesssim 1$ kpc. For distances $D_L \gtrsim 2$ kpc, the scale of the proper motion distribution is set by the ratio of Galactic $v_{\text{rot}}/R_0 = \mu_{\text{SgrA}^*} = 6.4 \text{ mas yr}^{-1}$. But at nearby distances, $D_L \lesssim 2$ kpc, the local transverse stellar velocities $\sigma_\perp \sim 37 \text{ km s}^{-1}$ divided by the distance, $\mu_{\text{loc}} = \sigma_\perp/D_L = 7.8/(D_L/\text{kpc}) \text{ mas yr}^{-1}$, must be added in quadrature. These higher proper motions for nearby lenses are relevant because, formally, the sensitivity of the LEO approach is restricted

to $D_L < 3.2$ kpc, and only opens up to a dex of mass range for $D_L < 1.3$ kpc. See Figure 3. As mentioned above, the sensitivity of LEO observations to parallax is greatly affected by whether or not significant magnification persists on both sides of an occultation, or preferably, for at least one orbit, i.e., 90 min. At the magenta (“Paczynski limit”) boundary, i.e., $\rho = 2$, the significantly magnified region does not extend much beyond the face of the source, whose diameter in this illustration is $2\theta_* = 0.6 \mu\text{as}$. Hence, to be magnified for one orbit requires $\mu_{\text{rel}} \lesssim 2\theta_*/90 \text{ min} = 3.5 \text{ mas yr}^{-1}$. Such slow proper motions are relatively rare when the characteristic proper motions are $\mu_{\text{rel}} \sim 6 \text{ mas yr}^{-1}$, but become much rarer for the higher values at $D_L \lesssim 1$ kpc.

The third issue (which goes in the opposite direction of the second), is that for LEO, the true limit on the measurability of parallax may be closer to the “Detection limit” (blue line) than the “Paczynski limit” (magenta line). As discussed by Gould et al. (2024), the reason that $\rho \gg 1$ events present difficulties for the two-observatory (Refsdal 1966) parallax method is that the Paczynski parameters must be separately measured from each site, and Johnson et al. (2022) showed that this is can be very difficult for $\rho \gg 1$. However, parallax measurements that rely on the acceleration of a single site, such as AP (Gould 1992), GEO (Gould 2013a), and LEO (Honma 1999), might not face an analogous restriction. This is particularly the case in the region between the magenta and blue lines (and for nearby lenses) because π_E can be very large, leading to very large deviations from rectilinear motion as seen from LEO.

For all these reasons, the efficacy of LEO-only parallax measurements must be addressed by simulations. These simulations will determine whether *CSST*, which is already selected for launch, can be usefully employed for FFP parallaxes, but they can also guide the design of new LEO missions that have FFP parallaxes as one of their mission goals.

6. Discussion

To my knowledge, there is only one survey mission that is already planned for either GEO or LEO, namely *CSST*. Because this is a LEO mission, no complementary ground-based observations are required to obtain parallaxes. Hence, the only issue is to determine whether observations based on the existing design will yield good FFP π_E measurements.

However, for future LEO and GEO missions that have FFP parallaxes as one of their mission goals, the design issues extend much more broadly than have been explored in this work. As one example, GEO is 40 times closer to Earth’s surface than L2, meaning that 1600 times less bandwidth is required for the same data download. This opens the

possibility of using vastly larger detector arrays relative to the L2 surveys, *Roman* and *Euclid*, which in turn might require using optical CCDs rather than infrared arrays, simply due to cost. Related to this is the issue of telescope aperture. For fixed focal design, the sky area scales inversely with the aperture, so that (ignoring slew/readout time and sky/field-star background) one can reach the same signal-to-noise ratio by observing a single field using a smaller aperture or tiling through several smaller fields with a larger aperture. The two caveats just mentioned (readout and sky) work in opposite directions, and so plausibly roughly cancel. However, smaller-aperture telescopes are vastly cheaper, and (given the less severe bandwidth requirements just mentioned) one might consider putting several such smaller telescopes on the same spacecraft bus, in analogy to the approach pioneered by ground-based transit surveys.

It is not my intention to explore all such issues in the present work. I merely point out that the problem of FFP parallaxes in the dwarf planet regime should be thought through from the bottom up.

I thank Subo Dong for valuable comments and suggestions.

REFERENCES

- Bachelet, E. & Penny, M. 2019, *ApJ*, 880, L32
- Bachelet, E., Specht, D., Penny, M., et al. 2022, *A&A*, 664, 136
- Ban, M. 2020, *MNRAS*, 494, 3235
- Ge, J., Zhang, H., Zang, W., et al. 2022, arXiv:2206.06693
- Gould, A. 1992, *ApJ*, 392, 442
- Gould, A. 1994, *ApJ*, 421, L75
- Gould, A. 1997, *ApJ*, 480, 188
- Gould, A., Gaudi, B.S. & Han, C. 2003, *ApJ*, 591, L53
- Gould, A., Udalski, A., Monard, B. et al. 2009, *ApJ*, 698, L147
- Gould, A. 2013a, *ApJ*, 763, L35
- Gould, A. 2013b, arXiv:1304.3455

- Gould, A. 2016, JKAS, 49, 123
- Gould, A. 2020, JKAS, 53, 99
- Gould, A., Zang, W., Mao, S., & Dong, S., 2021, RAA, 21, 133
- Gould, A., Jung, Y.K., Hwang, K.-H., et al. 2022, JKAS, 55, 173
- Gould, A., Yee, J.C., & Dong, S. 2024, arXiv:2406.14531
- Holz, D.E. & Wald, R.M. 1996, ApJ471, 64
- Honma, M. 1999, ApJ, 517, L35
- Johnson, S.A., Penny, M., Gaudi, B.S., et al. 2020, AJ, 160, 123
- Johnson, S.A., Penny, M., & Gaudi, B.S. 2022, ApJ, 927, 63
- Mogavero, F.& Beaulieu, J.-P. 2016, A&A, 585, A62
- Paczynski, B. 1986, ApJ, 304, 1
- Refsdal, S. 1964, MNRAS, 128, 295
- Refsdal, S. 1966, MNRAS, 134, 315
- Sumi, T., Koshimoto, N., Bennett, D.P., et al. 2023, AJ, 166, 108
- Yan, S. & Zhu, W. 2022, RAA, 22, 025006
- Yee, J.C., Udalski, A., Sumi, T. et al. 2009, ApJ, 703, 2082
- Zhu, W. & Gould, A. 2016, JKAS, 49, 93
- Zhu, W., Udalski, A., Huang, C.X. et al. 2017, ApJ, 849, L31

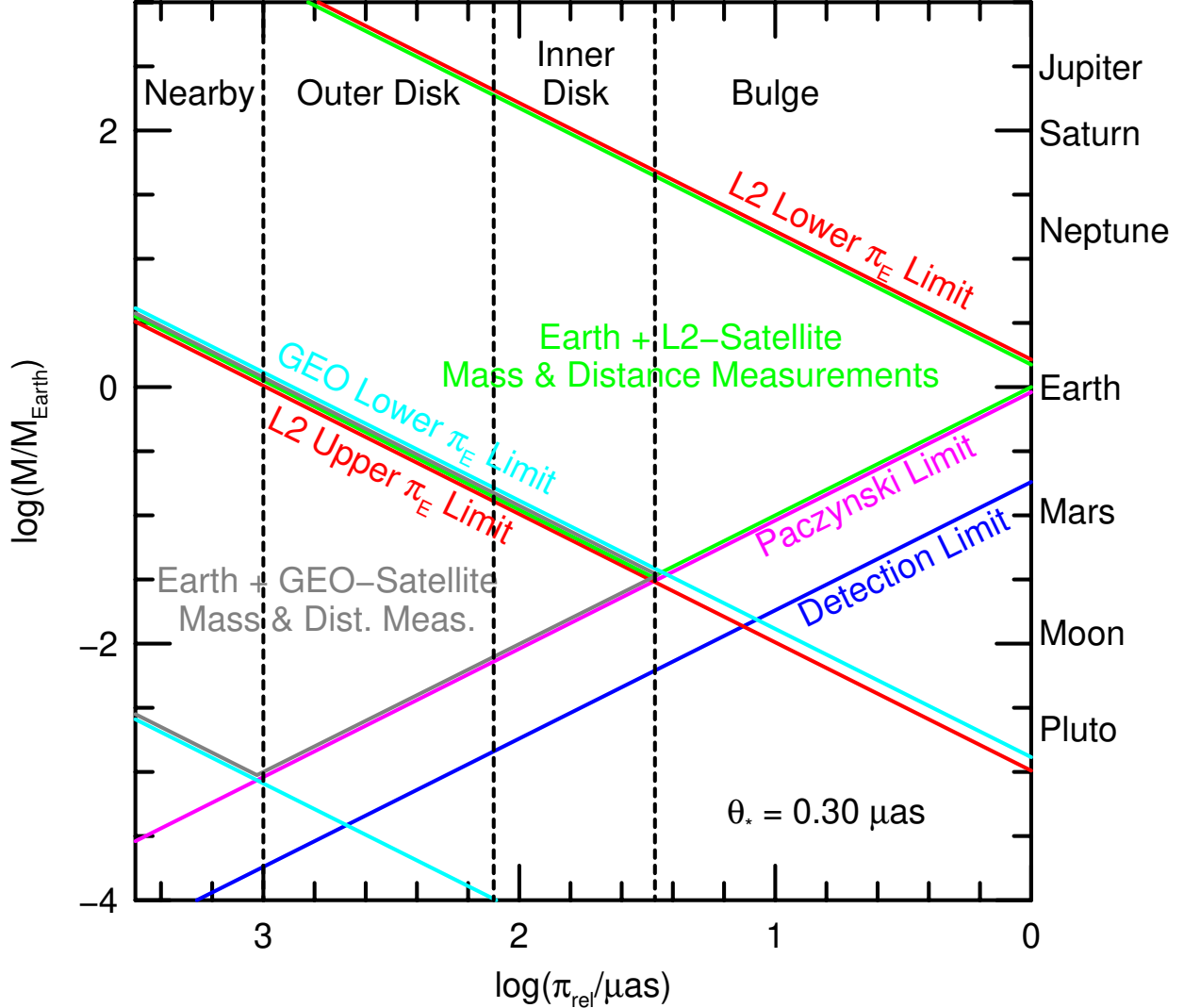


Fig. 1.— Extended version of Figure 4 from Gould et al. (2024), which focused on parallax measurements derived from two observatories separated by the Earth-L2 distance (0.01 au). The red, green, magenta and blue lines are identical to that Figure. The cyan and gray lines are new. These illustrate the regions of parallax-measurement sensitivity based on observatories separated by the Earth-GEO distance on the FFP-mass/ π_{rel} plane. Above the top cyan line, the two observatories see essentially the same event, while below the bottom cyan line, one observatory will not see the event at all. Below the magenta line, the Paczyński (1986) parameters cannot be measured, which undermines the π_E measurement according to Equation (6). π_E measurements can therefore be made within the gray contours. These reach to substantially lower FFP masses compared to Earth-L2 observations, but are restricted to the Galactic-disk FFPs (vertical lines).

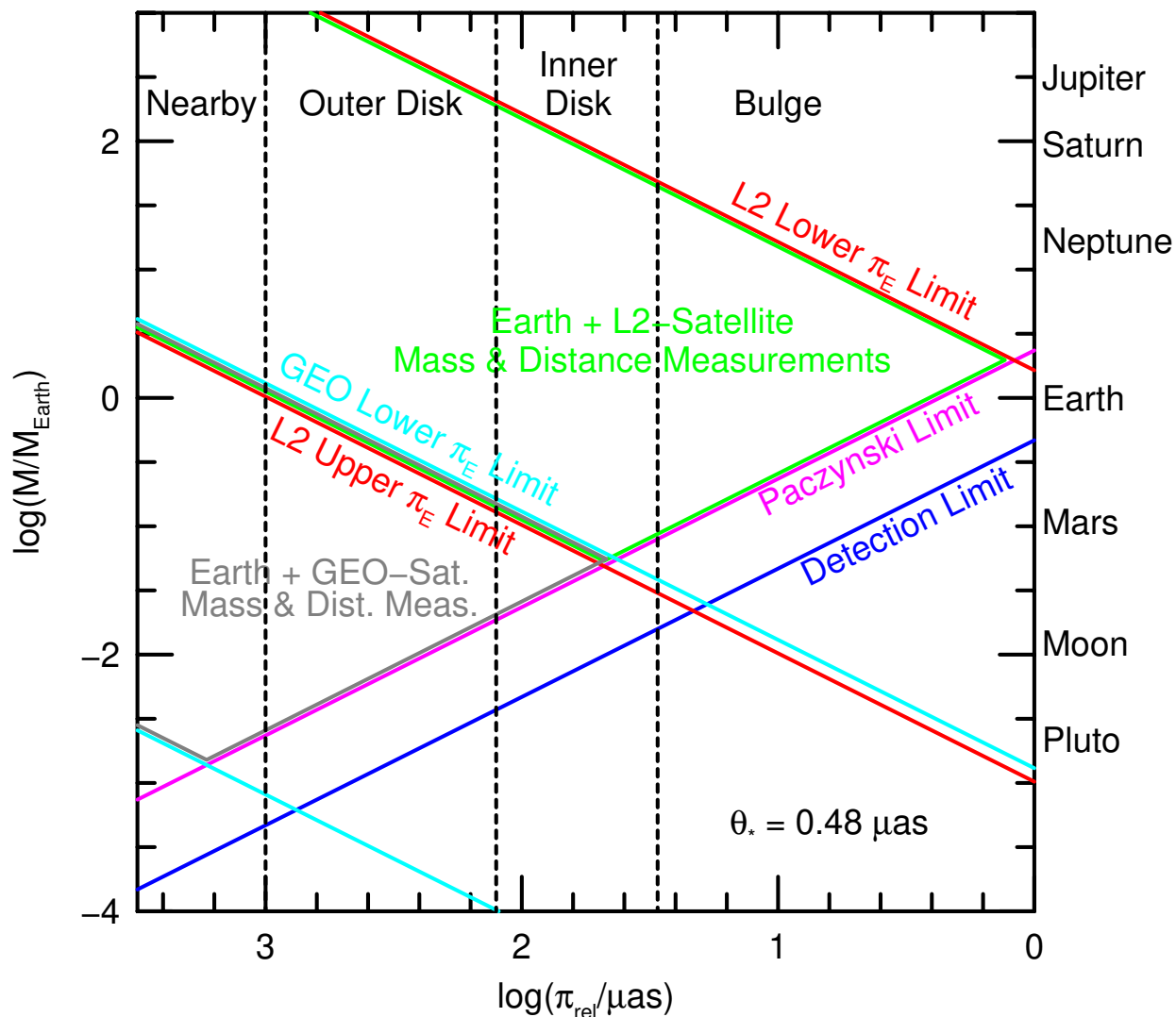


Fig. 2.— Same as Figure 1 except that the blue and magenta lines are drawn under the assumption of an early K-dwarf source ($\theta_* = 0.48 \mu\text{as}$) rather than an early M-dwarf source ($\theta_* = 0.30 \mu\text{as}$). The regions of sensitivity of both Earth-L2 and Earth-GEO observations are reduced compared to Figure 1. Figure 1 is more appropriate if the “Earth” observatory is a spacecraft in LEO orbit or LSST on the ground, while this Figure is more appropriate for typical ground-based survey telescopes.

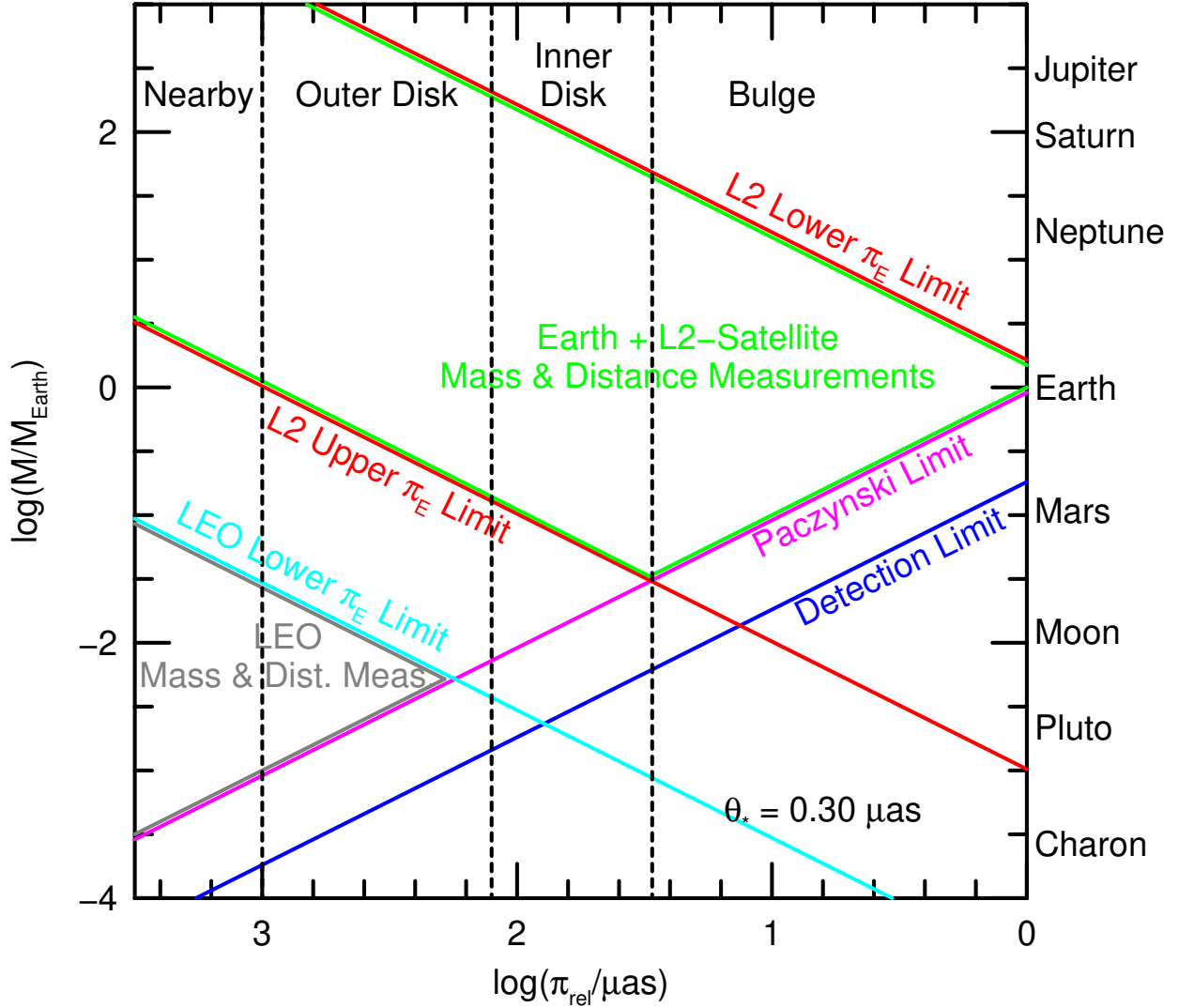


Fig. 3.— Rough representation of the M - π_{rel} space that is accessible to FFP parallax measurements from LEO. The Figure is constructed simply by substituting $D_{\perp} = a_{\text{LEO}} = 1 R_{\oplus}$ for $D_{\perp} = a_{\text{GEO}} = 6.6 R_{\oplus}$ in Figure 1. Comparing to that Earth-GEO Figure, the LEO-only observations reach to even lower FFP masses but are restricted to even more nearby populations. As discussed in Section 5, several aspects of this Figure require deeper investigation based on simulations, so it should be regarded as a very rough guide to what is possible.